

# Resource Allocation Management System for Interference Mitigation in Femtocell Networks

1 Latha.R 2 Sivaramkrishnan.S

1Assistant Professor 2 PG Scholar

1, 2 Master of Computer Application

1, 2Vel Tech High Tech Dr. Rangarajan Dr. Sakunthala College of Engineering,  
Chennai, India.

**Abstract** - One of the helpful techniques of improving the coverage and enhancing the capacity and resource allocation in cellular wireless networks is to reduce the cell size and transmission distances. The concept of deploying femtocells over macro cell has recently concerned growing interests in academic circles, industry, and consistency forums. Various technical challenges towards group deployment of femtocells have been address in recent creative writing. Interference mitigation femtocell and macro cell is considered to be one of the major challenges in femtocell networks because femtocells share the same permitted frequency spectrum with macrocell the different state-of-the-art approaches for interference and resource management in orthogonal frequency-division multiple access (OFDMA)-based femtocell networks. We develop a local searching algorithm and pareto optimal matching algorithm for using the project.

**Index Terms**— Femtocells, power control (PC), resource allocation (RA), outage balancing, interference management, orthogonal frequency division multiple access (OFDMA).

## I. INTRODUCTION

Low-Power low-cost femto base-stations (FBS) have shown promises for providing better indoor/dense coverage and higher system throughput. Allowing femtocells to share the channels with macro-cell user equipments (MUE) can offer better spectral efficiency, but unplanned femtocell deployment may significantly degrade system performance. In this paper, we study the problem of outage balancing in a tiered multi-carrier macro-femto network through joint resource allocation (RA) and power control (PC). power control problem formulations with each sub-problem transformable to a geometric programming problem. The generalization to a multi-carrier system, however, is non-trivial due to the intrinsic non convexity when dealing with interference channel and the combinatorial nature of RA. Joint PC and RA (JPCRA) algorithms have been proposed in [9]–[12]. As its single carrier counterpart, solutions to multi-carrier multi-cell JPCRA problems are generally NP-hard. [9] proposed a heuristic cluster-based JPCRA algorithm to tackle a multi-objective problem considering users' differential QoS requirements. Linear approximation is applied by [10] to transform the rate maximization problem into a

mixed integer linear programming, requiring full channel knowledge at a central node. In [11], dual decomposition is used to separate different optimizing variables. Main contributions of this paper can be summarized as follows: (1) From known channel statistics, we formulate the outage-balancing of femtocells into a (non-convex) optimization problem under the macrocell user outage probability constraint. We apply successive convex approximation (SCA) to find an approximate solution to the outage-balancing problem and provide a local searching algorithm by solving a sequence of geometric programming (GP) problems. A practical distributed implementation of the outage balancing problem by utilizing some message passing among base-stations over the network back-haul links. The following notation is used in our paper. Column vectors and matrices are denoted by boldfaced lowercase and uppercase respectively. Let  $\rho(F)$  denote the Perron-Frobeniuseigen value of a nonnegative matrix  $F$ , and  $x(F)$  and  $y(F)$  denote the Peron right and left eigenvectors of  $F$  associated with  $\rho(F)$ . We let  $e_i$  denote the unit coordinate vector,  $I$  denote the identity matrix and  $\mathbf{1} = [1, \dots, 1]$ . The superscripts  $(\cdot)^T$  denotes transpose, and  $\|\cdot\|_F$  denotes the Frobeniusnorm. We denote  $x \circ y$  as a Schur product of  $x$  and  $y$ , i.e.  $x \circ y = [x_1 y_1, \dots, x_L y_L]$ . For a vector  $x = [x_1, \dots, x_L]$ ,  $\text{diag}(x)$  is its diagonal matrix  $\text{diag}(x_1, \dots, x_L)$ . Let  $e_x$  denote  $e_x = (e_{x1}, \dots, e_{xL})$ , and  $\log x$  denote  $\log x = (\log x_1, \dots, \log x_L)$ . An equality involving eigen vectors is true up to a scaling constant. the RA scheme for one cell does not affect the optimal function value. Unless otherwise specified, we locate the  $m$ -th channel to such are power constraints for all BS and  $P_i$  is the total power budget. Constraint (3d) implies that exactly one channel is allocated to one user. Linear constraint (3e) ensures that one channel can be allocated to at most one user by assumption. In what follows, we will describe a SCA algorithm to find (at least) a local optimal point to problem (12) by solving a series of GP problems. where  $w_i$ ,  $m$  is the relative importance of the FUE- $(i, m)$ 's success probability and  $\tau_{0,m}$  is a pre-specified constant that represents the maximal allowed outage probability for the  $m$ -th MUE. Since the channel statistics are channel independent by A.2, fixing the RA scheme

for one cell does not affect the optimal function value. Unless otherwise specified, we allocate the  $m$ -th channel to MUE- $m$  such that  $C(m)_{0,m} = 1$ . In our problem formulation, the two parameters related to PBSs or PUs are channel gains between SUs and PBSs (i.e.,  $g_{ij}$ ), and interference levels caused by PUs to the SBS (i.e.,  $I_P$ ). Estimating and tracing the exact values of the above parameters are not easy for SUs due to the fact that PBSs are not obliged to provide any information to SUs. Both of the above parameters are contained in the linear constraints C2 and C3 in (4). To deal with such uncertainties, we use the worst case robust optimization method for affine constraints convex optimization. Orthogonal RA is assumed among UEs in each cell (macrocell or femto-cell) such that there is no co-channel interference between users served by the same BS. A cell is the service area covered by a BS. Together with A.5, we further restricts the number of users  $M_i \leq K, \forall i \in B$  to ensure RA feasibility. Let  $C(k)_{i,m}$  be an indicator of channel allocation with  $C(k)_{i,m} = 1$  if channel  $k$  is allocated to user  $(i, m)$  and zero otherwise. If user  $(i, m)$  is allocated channel  $k$ , the received SINR.

## II. POWER CONTROL RESOURCE ALLOCATION

We consider a heterogeneous network configuration in which femtocells share macro-cell channels. Assuming that interference from other macro-cells are well-mitigated, we confine the interference effect and outage balancing problem within one macro-cell. Our problem formulations are based on the following assumptions: A.1 Independent Rayleigh fading is assumed for all channel links. A.2 Denote the mean channel power gain from BS- $j$  to user  $(i, m)$  as  $G_{ij,m}$  and fast fading term as  $g(k)_{ij,m}$  in channel  $k$ . Then the instantaneous channel power gain is  $G_{ij,m} g(k)_{ij,m}$  with  $g(k)_{ij,m}$  satisfying exponential distribution with unit mean because of assumption A.1. A.3 We assume that both  $G_{ij,m}$  and noise power  $n_{i,m}$  at UE  $(i, m)$  are independent on channel  $k$ . A.4 Let  $p(k)_i$  be the transmit power of BS- $i$  in channel  $k$ . We assume that the average interference power  $\{p(k)_j G_{ij,m}, j \neq i\}$  and channel  $G_{ij,m}$  can be measured at user  $(i, m)$ . A.5 Every MUE or FUE is allocated only one channel. This is assumed for simplicity of presentation. When a single UE is allocated multiple channels with per-channel SINR requirement, the UE can be modeled as multiple virtual users, each with one channel. The SINR thresholds for FUEs, on the other hand, are variables in our problem formulation. This SINR distribution is translated to a rate allocation through Shannon's capacity formula as in the left hand-side of (5c) and  $R_i$  is the rate threshold. For simplicity, ideal capacity formula is used in this paper for the FUE rate calculation, though modulation and

coding gaps can also be included depending on the practical transmission schemes. As such, the robust power allocation problem is changed to the standard form of convex optimization, which can be solved very efficiently. 1. Algorithm 1 Main Iteration Step 1: Initialize  $s = 1, a(k)_{j,s} = 1$  for  $\forall j \in F, b(k)_s = 0$  for  $\forall k \in K_0$  and a feasible  $p_0 = \{p(k)_i, 0\}$  Step 2: Find optimal solution  $p_s = \{p_i, s\}$  to problem (15) Step 3:  $s \leftarrow s+1$ ; updates  $a(k)_{j,s}$  and  $b(k)_s$  using (13) and (14). Go to Step 2 unless stopping criterion is met. Proposition 1

The convergence follows from the general results for the generic convex approximation methods [25]. Convexity of the transformed problem (10) implies the convergence to an optimal point.

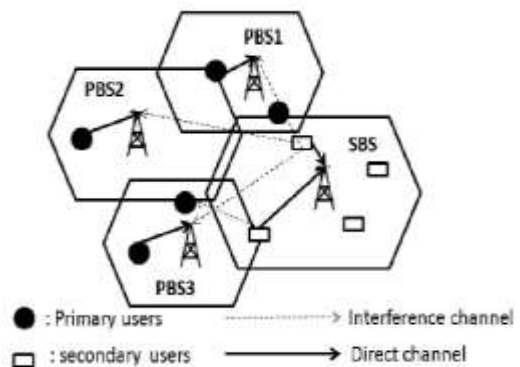


Fig. 1. A cellular CRN with primary and secondary users.

## III. LOCAL SEARCHING ALGORITHM

In many optimization problems, the state space is the space of all possible complete solutions. We have an objective function that tells us how "good" a given state is, and we want to find the solution (goal) by minimizing or maximizing the value of this function. In many optimization problems, the state space is the space of all possible complete solutions. We have an objective function that tells us how "good" a given state is, and we want to find the solution (goal) by minimizing or maximizing the value of this function. The start state may not be specified. The path to the goal doesn't matter. In such cases, we can use local search algorithms that keep a single "current" state and gradually try to improve it.

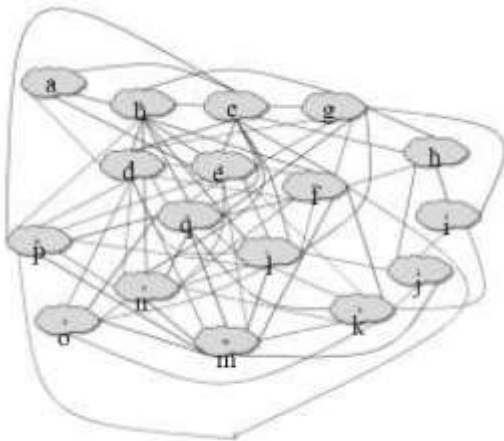
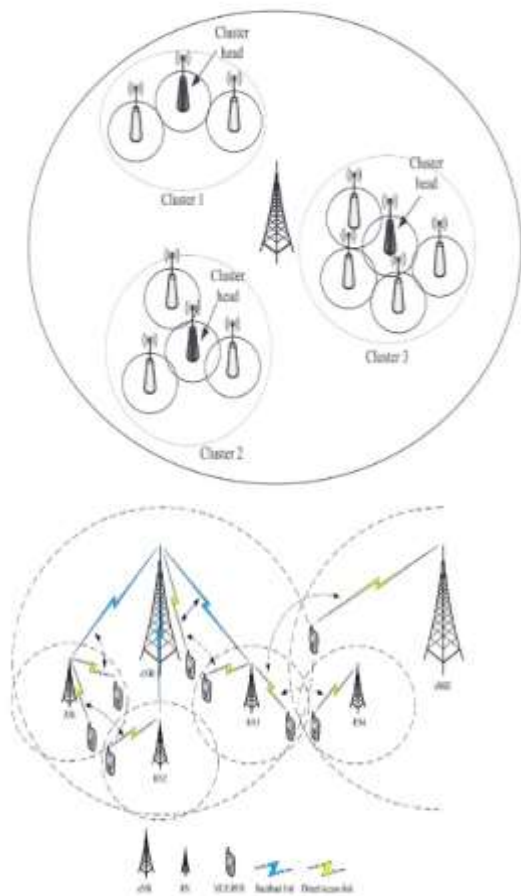


Figure 4. Algorithm 1, step 2: The graph  $G'$

#### IV. PARETO OPTIMAL MATCHING ALGORITHM

Fix  $N = \{1, \dots, n\}$ , a set of agents and  $H$ , a set of equally many objects, called houses. A sub matching  $\mu : N \rightarrow H$  is a bijection with  $N \setminus \mu(N)$  and  $H \setminus \mu(N)$ ;  $\mu(i)$  is agent  $i$ 's match under  $\mu$ . If  $N \setminus \mu(N) = \emptyset$ ,  $\mu$  is a matching. Matchings are also denoted as vectors with the understanding that the  $i$ th component of  $\mu$  represents  $\mu(i)$ . The sets of all matchings and respectively of all sub matchings that are not themselves matching, are  $M$  and  $M'$ . The sub matching under which no one is matched,  $\emptyset$ , is an element of  $M'$ . The sets of unmatched agents and houses at some  $\mu \in M$  are  $N \setminus \mu(N)$  and  $H \setminus \mu(N)$ . If  $\mu(i) = \mu_0(i)$  for all  $i \in N \setminus N_0$  holds for two sub matchings  $\mu, \mu_0$ , then  $\mu$  is a sub matching of  $\mu_0$  ( $\mu \leq \mu_0$ ). Pycia and Unver's [10] ingenious terminology to define Papai's [28] hierarchical exchange mechanisms. For any  $\mu \in M$  define an ownership function  $o_\mu : H \rightarrow N$ , with the understanding that agent  $o_\mu(x)$  owns house  $x$  at the sub matching  $\mu$ . A hierarchical exchange mechanism is defined through a set of ownership functions  $o = (o_\mu)_{\mu \in M}$  where  $o_\mu(x) = o_{\mu_0}(x)$  holds for any two sub matchings  $\mu \leq \mu_0$  with  $o_\mu(x) \in N_0$  and  $x \in H_0$ . So ownership must persist in the sense that an agent  $i \in N_0$  must own a house  $x \in H_0$  at  $\mu_0$  if  $i$  owns  $x$  at a sub matching  $\mu$  of  $\mu_0$ . The outcome of any hierarchical exchange mechanism is determined through the following trading process. At the start let  $\mu_1 = \emptyset$ ; and  $k = 1$ . Round  $k$ : each house in  $H \setminus \mu_k(N)$  points to its owner according to  $o_{\mu_k}$ , each agent  $i \in N \setminus \mu_k(N)$  points to a house in  $H \setminus \mu_k(N)$ . At least one cycle forms. Calculate  $\mu_{k+1}$  as  $\mu_{k+1}(i) = \mu_k(i)$  for  $i \in N \setminus \mu_k(N)$  and  $\mu_{k+1}(i) = x$  if  $i$  points to  $x$  in one of the cycles. Terminate the mechanism if  $\mu_{k+1}$  is a matching. If not, go on to round  $k + 1$ . At the start of a hierarchical exchange mechanism, agents are asked to point to houses. Houses in turn point to their owners. At least one cycle of agents and houses forms. Any agent in such a cycle is matched with the house he is pointing to and leaves the mechanism. When an

owner of multiple houses leaves, his unmatched houses are passed on to the remaining agents according to some  $\mu$ -inherited rule, implied by the ownership functions. Agents are once again asked to point to the remaining houses and the same procedure is repeated until each. The restriction to hierarchical exchange mechanisms is not costless. Pycia and Unver [30] define a class of problems in which hierarchical exchange mechanisms are strictly Lorenz-dominated by some other strategy proof, Pareto optimal and non-bossy mechanisms. Abdul kadiroglu, Cheand Yasuda [3] show that the use of ordinal mechanisms when agents have cardinal utilities may lead to welfare losses, Pycia [31] shows that these losses can be arbitrarily large. Agent is matched. Serial dictatorships  $\mu^o$  and Gale's top trading cycles mechanism by Shapley and Scarf [33]) are hierarchical exchange mechanisms. The former arises when  $\mu^o(h)$  only depends on  $j \in N \setminus j$  the number of agents already matched under  $\mu$ , the latter arises if  $o_\mu(h) \neq o_{\mu_0}(h)$  holds for all  $h \in H_0$ . For any  $\mu \in M$  define a hierarchical exchange mechanism and any permutation  $p : N \rightarrow N$  define a permuted hierarchical exchange mechanism. From assumptions A.1 to A.3, the numerator is the instant angelus received signal power from the serving BS- $i$ , while the denominator contains interference from other BS's and the noise power at the receiver. To simplify the notation, define  $F_{i,j,m} = G_{i,j} \cdot \mu_{i,m} / G_{i,i,m} \cdot \nu_{i,m} = \nu_{i,m} / G_{i,i,m}$ . success probability and  $\epsilon_{0,m}$  is a pre-specified constant that represents the maximal allowed outage probability for the  $m$ th MUE. Since the channel statistics are channel independent by A.2, fixing the RA scheme for one cell does not affect the optimal function value. the outage performance versus the main iteration number  $s$ . While we would rather not waste computation for a sub-problem by choosing  $T$  so large that the algorithm already converges for each sub problem before updating, larger  $T$  is in general more preferable than updating the coefficients and moving to another sub-problem prematurely for smaller final convergence error.



Denote the set of resources and the set of femtocells (and their FBS) as  $K = \{f_1, \dots, f_K\}$  and  $N = \{f_1, \dots, f_N\}$ , respectively. Let the index of MBS be 0 and the total set of base stations be denoted as  $B = N \cup \{0\}$ . We further assume that resources are shared in TDMA mode within each femtocell such that at a given time, only one FUE will be scheduled, while multiple non-interfering MUEs can be scheduled at the same time. The resource allocation and SINR requirement for each macro-cell user equipment (MUE) remains stationary with in the time-duration of femtocell action, in which FBS's can dynamically distribute its SINR requirements in different resources to satisfy the FUE's downlink rate requirement. In order to achieve user service fairness, this work considers the problem of outage balancing among actively connected FUEs in a spectrum sharing heterogeneous system. Our approach aims to minimize a utility function of outage probability of FUEs under constraint of MUE outage requirement. This SINR distribution is translated to a rate allocation through Shannon's capacity formula as in the left-hand-side of (5c) and  $R_i$  is the rate threshold. For simplicity, ideal capacity formula is used in this paper for the FUE rate calculation, though modulation and coding gaps can also be included depending on the practical

transmission schemes. (5d) denotes the total power constraint with  $P_i$  is the power budget for the  $i$ th BS. Assuming a full resource sharing scenario of  $K = 5$ , Fig.3 shows each FUE's outage probability versus different rate requirement for two configurations. As FBS 3 moves from lower left to upper left, it causes more interference to FBS 2 and also sees higher interferences from other nodes.

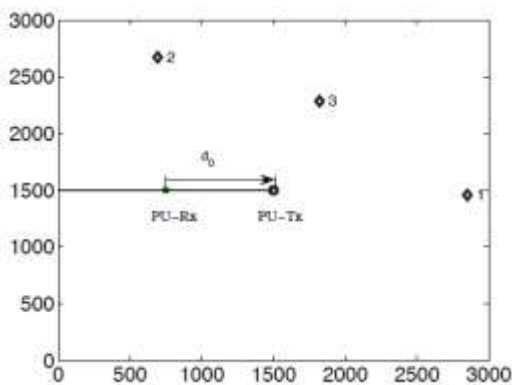
TABLE I: System Parameters

Noise Power Spectral Density $N_0$	-174 dBm
MBS antenna gain	18 dBi
Wall penetration loss $\rho$	10 dB
FBS and user antenna gain	0 dBi
Distance between FBS and FUE	{25m, 35m}
Bandwidth of a resource block $W$	1.08MHz
Maximum MBS transmit power $P_{tot}$	43 dBm
Maximum FBS transmit power $P_{max}$	20 dBm
Path-loss from MBS to MUE (distance $r_m$ )	$15.3 + 37.6 \log_{10}(r)$
Path-loss from MBS to FUE (distance $r_m$ )	$15.3 + 37.6 \log_{10}(r) + \rho$
Path-loss from FBS to FUE in the same femto-cell (distance $r_m$ )	$38.46 + 20 \log_{10}(r)$
Path-loss from FBS to FUE in other femto-cell (distance $r_m$ )	$\max\{15.3 + 37.6 \log_{10}(r), 38.46 + 20 \log_{10}(r) + 2\rho\}$
MUE rate requirement	$20 W = 21.6 \text{ Mbit/s}$
MUE outage requirement	0.1
Weights $w_i$	Uniform

### V. SIMULATIONS

In this section, we present simulation studies on the performance of the proposed DDPC algorithm in the case of multiple asynchronous SU's. First, we provide the convergence result for the special case in which the observation noise additive to  $\tilde{g}(\Lambda)$  is a zero-mean uniformly distributed random variable within  $[-0.5, 0.5]$ . In the simulation, we set  $M = 3$ ,  $\eta = 0.1, \eta_0 = 0.01$ ,  $c = 0.0001$ ,  $v = 0.4$ ,  $a_0 = 50$ , and  $P_{max} = 30\text{dB}(1000\text{mW})$  (the corresponding  $\bar{x} = \log(1000) = 6.9078$ ). The activation instants of the three SUs are 1, 100, and 200, respectively. The initial value of  $\lambda_i(0)$  is set to 100 for each SU. The effective interference channel gain from each SU to the PU-Rx  $b$  is set to  $[0.3568, 0.0197, 0.4432] \times 10^{-3}$ . In other words, SU-2 has the best channel opportunity. We display the updates of  $\lambda_i$  and  $x_i$  over time, and the convergent point  $\lambda_s$  in Figure 4, from which we can confirm the convergence of more than two SUs without synchronization. After convergence, the transmit power of SUs is [112, 1000, 90] mW. Specially, SU-2 transmits with the maximum power most of the time. We can observe that SUs with larger average interference channel gains transmit with smaller power. We also test the algorithm using 5 different random seeds, and the resulting average ePU outage probabilities along each convergence process are smaller than 0.1004, i.e., only slightly larger than  $\eta$ . We also show the difference between the convergent point  $\lambda_s$  and  $\lambda_0$  as the value of  $c$  varies in Figure 5 for cases when  $M = 2, 4, 6$ ,  $\eta = 0.1$ , and  $\eta_0 = 0.01$ . We can observe that, as  $c$  increases, the difference increases. In addition, more SUs in the system lead to larger difference.

The PU outage probability normalized by  $\eta$  after convergence and its upper bound derived in (42) are also shown for comparison in Figure 6. We can see that by setting  $c$  small enough, the resulting PU outage probability is very close to its requirement. The result also indicates that, for a larger value of  $c$ , it may be helpful to have an outer loop to adjust the value of  $\eta u$  as in Figure 2 to satisfy the original target protection constraint defined by  $\eta$ . Another way to guarantee that the PU outage probability is below the predefined threshold  $\eta$  along the convergence process is to use large enough initial points  $\lambda_i(0)$  (but smaller than  $\bar{\lambda} = 1/c \log(1/\eta)$ ) such that the update of  $\lambda_i(k)$  is bounded. Next, we evaluate the performance of our proposed DDPC in a more practical setting. We set up a system with multiple SU pairs and one PU pair with their locations shown in Figure 3. For SUs, only the transmitters are shown.



The duration for one outage probability update is set to  $T = 200$ . Note here that the noise caused by the estimation of (26) is biased. To test the proposed algorithm under a more dynamic system, we also allow the distance of the PU-Rx from the PU-Tx ( $d_0$ ) to jump from 500 meters to 600 meters at the middle of the simulation outage. As a result, the outage probability perceived by the PU-Rx without SU transmission changes from  $\eta_0 = 0.0186$  to  $0.0381$  and the margin for SU transmission is reduced. In Figure 7, we plot update process of the “Lagrangian multiplier”  $\lambda_i$  for  $\eta u = 0.10$ . We can observe the convergence behavior of the proposed algorithm. Although we encounter noisy observations/estimations during outage sensing, the algorithm converges smoothly and fairly as each SU eventually acquires similar value of  $\lambda_i$ . Also note that there exists a small gap between the convergent point and  $\lambda^*$ . This difference is caused by the bias in the estimation of the outage probability (in log-scale). This gap can be reduced by adopting a longer observation period, i.e., a greater  $T$ . However, this may render the update less agile and less sensitive to the system dynamics. In Figure 8, we plot the outage probability perceived by the PU as a function of

time by setting  $\eta u = 0.10$  and  $\eta u = 0.09$  for our DDPC algorithm. Note that the time index in Figure 8 aligns with that in Figure 7. In other words, the outage probability shown is along the convergence process. We can observe that with  $\eta u = 0.10$ , the outage probability perceived by the PU over the whole simulation time is only slightly higher than required. As discussed earlier, this offset can be overcome by applying an outer-loop control mechanism to adjust the target outage probability requirement  $\eta u$  in place of  $\eta$  used in our algorithm. This is confirmed by observing that the PU outage probability is under the constraint almost all the time with  $\eta u = 0.09$ . In Figure 9, we show the total SU utility  $\sum \log(1 + h_i P_i)$  achieved by the DDPC algorithm as a function of time  $100\lambda_i$  time. To test at the middle of the simulation the proposed algorithm under a more dynamic system, we also allow the distance of the PU-Rx from the PU-Tx ( $d_0$ ) to jump from 500 meters to 600 meters outage. As a result, the outage probability perceived by the PU-Rx without SU transmission changes from  $\eta_0 = 0.0186$  to  $0.0381$  and the margin clearly if the graph  $G'$  is properly colored by the minimum number of colors, then the algorithm may set as few elements as possible to the edges of  $G'$ , since that coloring of  $G'$  ensures that the same elements are set properly as many times as possible. Unfortunately, the problem of properly coloring the vertices of an undirected graph with the minimum number of colors, is known to be NP-hard [11], that is, mathematicians believe that no polynomial time algorithm exists for solving that problem. We believe that this is also the status of our proposed Resources Allocation Problem.

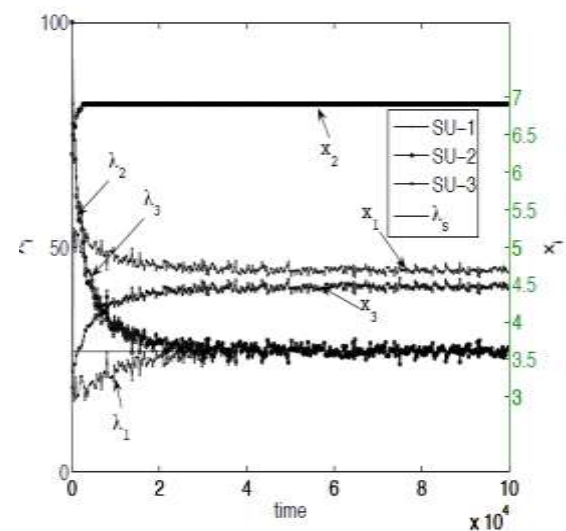


Fig. 4. Convergence behavior of the proposed DDPC algorithm with noisy Observation.



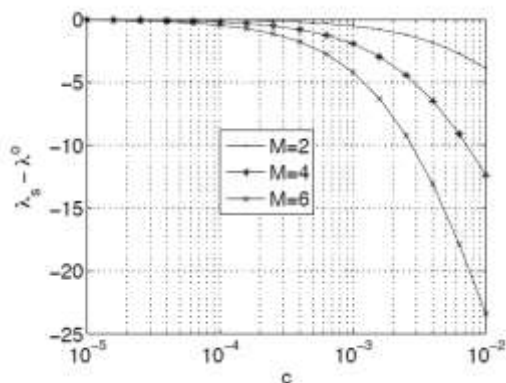
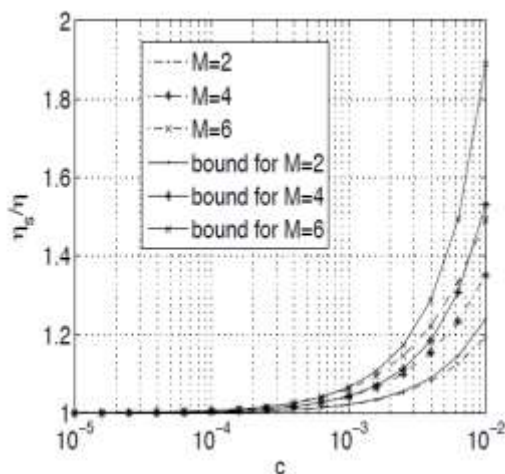


Fig. 5. Difference between the convergent point  $\lambda_s$  and the optimal Lagrangian multiplier  $\lambda_o$ . For comparison, we plot the maximum SU utility of the transformed convex optimization problem (9) obtained by utility function approximation. We also plot the lower and upper bounds on the true optimal total SU utility of the original optimization problem (5) achieved by transforming the outage probability constraint using the certainty-equivalent margin (CEM) model as in [25] and [11]. The idea is to retain the  $\log(1+hiPi)$  utility function for each SU but use a lower/upper bound on the outage probability expression. The solutions to all the transformed convex optimization problems are obtained using the Mat lab-based convex optimization modeling system CVX [37]. We can see that the gap in the total utility achieved by the three approximation methods (utility approximation, lower bound and upper bound with CEM model) are negligible. We can also observe that the total utility achieved by the SUs with  $\eta_u = 0.10$  ( $\eta_u = 0.09$ ) may be slightly above (or below) the optimal utility for the original problem in (5). This is caused by the slightly higher (or lower) outage probability produced by the DDPC algorithm. The advantage of the DDPC lies in its distributed implementation.



The PBS is located at the center of a circular cell whose radius is 2 Km. The SBS is located 0.5 Km from the PBS and covers a circular cell with a radius of 1 Km. There are three active SUs in the cognitive cell, deployed at  $d = \{150, 200, 350\}$  m from SBS and  $D = \{550, 300, 400\}$  m from the PBS. The power range for each SU is  $\{0.001, 1\}$  Watts. Again, since we have only one PBS, we omit the index  $j$  from the notations.

**CONCLUSION**

In this work, we proposed a discounted distributed power control (DDPC) algorithm for multiple SUs in a cognitive radio network. The proposed algorithm exploits the outage information from the PU-Rx on the PU feedback channel as an external inference signal for coordination among distributed. We proved the convergence property of the proposed DDPC algorithm for two secondary user case, and provided the promising convergence results for scenarios with more than two SUs. This distributed SU power control can tackle synchronisness issue in a typical cognitive radio network and approximate the optimal solution without PU cooperation, central controller/monitor, or inter-SU message passing. In future works, we plan to generalize our frame work to include the more dynamic scenarios involving adaptive PU and SUs. We are also keen to assess the trade-off between the security concerns and the revenue from cognitive users by allowing some unencrypted link control feedback among the PU pairs.

**REFERENCES**

[1] C. Cordeiro, K. Challapali, D. Birru, and S. Shankar, "IEEE 802.22: An introduction to the first wireless standard based on cognitive radios," *Journal of Communications*, vol.1, no. 1, pp. 38–47, April 2006.  
 [2] Y. Yuan, P. Bah i, R. Chandra, P. A. Chou, J. I. Ferrell, T. Moscibroda, S. Narlanka, and Y. Wu, "Knows: Cognitive radio networks over whitespaces," in *IEEE DySPAN*, 2007, pp. 416–427.  
 [3] Q . Zhao and A. Swami, "A decision-the oreti framework for opportunistic spectrum access," *IEEE Wireless Commun. Mag.*, vol. 14, no. 4, pp.1536–1284, 2007.  
 [4] FCC, "Office of engineering and technology releases TV white space phase II testreport," <http://www.fcc.gov/oet/projects/tvbanddevice/Welcome.html>, Nov. 2008.  
 [5] 3GPP Technical Specification Group Radio Access Network Physical layer procedures (FDD) (Release 5), 3rd Generation Partnership Project Std. S25.214 V5.11.0, 2005.  
 [6] Wireless LAN Medium Access Control (MAC) and Physical Layer (PHY) Specifications: Higher-Speed Physical Layer Extension in the 2.4 GHz Band, ANSI/IEEE Std. 802.11b-1999 (R2003), 1999.  
 [7] G. Foschini and Z. Miljanic, "A simple distributed autonomous power control algorithm and its convergence," *IEEE Trans. Veh. Technol.*, vol. 42, no. 4, pp. 641–646, Nov 1993.

- [8] R. D. Yates, "A framework for uplink power control in cellular radio systems," *IEEE J. Sel. Areas Commun.*, vol. 13, pp. 1341–1347, 1996.
- [9] J. Huang, R. Berry, and M. Honig, "Distributed interference compensation for wireless networks," *IEEE J. Sel. Areas Commun.*, vol. 24, no. 5, pp. 1074–1084, May 2006.
- [10] M. Chiang, "Balancing transport and physical layers in wireless multihop networks: jointly optimal congestion control and power control," *IEEE J. Sel. Areas Commun.*, vol. 23, no. 1, pp. 104–116, Jan. 2005.
- [11] K. W. Choi, E. Hossain, and D. I. Kim, "Downlink sub channel and power allocation in multi-cell OFDMA cognitive radio networks," *IEEE Trans. Wireless Commun.*, vol. 10, no. 7, pp. 2259–2271, Jul. 2011.
- [12] D. T. Ngo, S. Khakurel, and T. Le-Ngoc, "Joint sub channel assignment and power allocation for OFDMA femtocell networks," *IEEE Trans. Wireless Commun.*, vol. 13, no. 1, pp. 342–355, Jan. 2014.
- [13] M. R. Javan and A. R. Sharafat, "Distributed joint resource allocation in primary and cognitive wireless networks," *IEEE Trans. Commun.*, vol. 61, no. 5, pp. 1708–1719, May 2013.
- [14] D. Nguyen and M. Krunz, "Spectrum management and power allocation in MIMO cognitive networks," in *Proc. IEEE INFOCOM*, Mar. 2012, pp. 2023–2031.
- [15] U. Krause, "Concave Perron–Frobenius theory and applications," *Nonlinear Anal., Theory, Methods Appl.*, vol. 47, no. 3, pp. 1457–1466, Aug. 2001.
- [16] U. Krause, "A local–global stability principle for discrete systems and difference equations," in *Proc. 6th Int. Conf. Difference Equations*, 2004, pp. 167–180.
- [17] B. Lemmens and R. Nussbaum, *Nonlinear Perron–Frobenius Theory*. Cambridge, U.K.: Cambridge Univ. Press, 2012.
- [18] H. Wang and Z. Ding, "Power control and rate allocation for outage balancing in femtocell networks," in *Proc. IEEE GLOBECOM*, Dec. 8–12, 2014.
- [19] C. W. Tan, "Optimal power control in Rayleigh-fading heterogeneous networks," in *Proc. IEEE INFOCOM*, 2011, pp. 2552–2560.
- [20] S. Huang, X. Liu, and Z. Ding, "Distributed power control for cognitive user access based on primary link control feedback," in *Proc. IEEE INFOCOM*, Mar. 2010, pp. 1–9.
- [21] S. Huang, X. Liu, and Z. Ding, "Decentralized cognitive radio control based on inference from primary link control information," *IEEE J. Sel. Areas Commun.*, vol. 29, no. 2, pp. 394–406, Feb. 2011.
- [22] C. Blum and A. Roli, "Metaheuristics in combinatorial optimization: Overview and conceptual comparison," *ACM Comput. Survey*, vol. 35, no. 3, pp. 268–308, Sep. 2003. [Online]. Available: <http://doi.acm.org/10.1145/937503.937505>
- [23] S. Kandukuri and S. Boyd, "Optimal power control in interference-limited fading wireless channels with outage-probability specifications," *IEEE Trans. Wireless Commun.*, vol. 1, no. 1, pp. 46–55, Jan. 2002.